Kidney360

Functionally Essential Tubular Proteins Are Lost to Urine-Excreted, Large Extracellular Vesicles during Chronic Renal Insufficiency

Ryan J. Adam,[1] Mark R. Paterson,[1] Lukus Wardecke,[1] Brian R. Hoffmann,[1,2,3,4] and Alison J. Kriegel[1,3,5]

Abstract

Background The 5/6 nephrectomy (5/6Nx) rat model recapitulates many elements of human CKD. Within weeks of surgery, 5/6Nx rats spontaneously exhibit proximal tubular damage, including the production of very large extracellular vesicles and brush border shedding. We hypothesized that production and elimination of these structures, termed large renal tubular extracellular vesicles (LRT-EVs), into the urine represents a pathologic mechanism by which essential tubule proteins are lost.

Methods LRT-EVs were isolated from 5/6Nx rat urine 10 weeks after surgery. LRT-EV diameters were measured. LRT-EV proteomic analysis was performed by tandem mass spectrometry. Data are available *via* the ProteomeXchange Consortium with identifier PXD019207. Kidney tissue pathology was evaluated by trichrome staining, TUNEL staining, and immunohistochemistry.

Results LRT-EV size and a lack of TUNEL staining in 5/6Nx rats suggest LRT-EVs to be distinct from exosomes, microvesicles, and apoptotic bodies. LRT-EVs contained many proximal tubule proteins that, upon disruption, are known to contribute to CKD pathologic hallmarks. Select proteins included aquaporin 1, 16 members of the solute carrier family, basolateral Na^+/K^+-ATPase subunit ATP1A1, megalin, cubilin, and sodium-glucose cotransporters (SLC5A1 and SLC5A2). Histologic analysis confirmed the presence of apical membrane proteins in LRT-EVs and brush border loss in 5/6Nx rats.

Conclusions This study provides comprehensive proteomic analysis of a previously unreported category of extracellular vesicles associated with chronic renal stress. Because LRT-EVs contain proteins responsible for essential renal functions known to be compromised in CKD, their formation and excretion may represent an underappreciated pathogenic mechanism.

KIDNEY360 1: 1107–1117, 2020. doi: https://doi.org/10.34067/KID.0001212020

Introduction

The kidney's proximal tubules (PTs), when healthy, reabsorb the majority of total glomerular filtrate, including large quantities of water, electrolytes, and nearly 100% of filtrate protein. Bulk reabsorption is enabled by the extensive surface area of apical microvilli, the so-called brush border, and their extensive reabsorption apparatus. Loss of the PT brush border has been reported in both acute kidney disease and CKD (1,2), and the pathologic effects of progressive brush border loss on renal function has been established in a mouse model of acute-to-CKD transition (3). The rat 5/6 nephrectomy (5/6Nx) remnant kidney model of CKD recapitulates many elements of human CKD, including brush border loss, proteinuria, albuminuria, polyuria, and more (1,3,4). We have observed the timing of brush border loss in these rats to coincide with renal functional decline, and with the presence of large extracellular vesicles originating from PTs (1). This process is distinct from AKI-associated brush border necrosis and sloughing. We term these vesicles large renal tubular extracellular vesicles (LRT-EVs). Despite our identification of what could be LRT-EVs published as histologic representations by other groups (with the earliest found dated 1914), we were unable to find explicit, in-text, literature reference to them, rendering their identification and functional consequence uncertain. LRT-EVs are too large to be exosomes (40–100 nm) or microvesicles (100–1000 nm) (5). Although the LRT-EV size range is compatible with apoptotic bodies (800–5000 nm) (5), there is no evidence of PT epithelial apoptosis *via* terminal deoxynucleotidyl transferase–mediated digoxigenin-deoxyuridine nick-end labeling (TUNEL) staining, and other methods, in our 5/6Nx model during the period of LRT-EV production.

[1]Department of Physiology, Medical College of Wisconsin, Milwaukee, Wisconsin
[2]Department of Biomedical Engineering, Medical College of Wisconsin, Milwaukee, Wisconsin
[3]Cardiovascular Center, Medical College of Wisconsin, Milwaukee, Wisconsin
[4]Max McGee National Research Center, Medical College of Wisconsin, Milwaukee, Wisconsin
[5]Center of Systems Molecular Medicine, Medical College of Wisconsin, Milwaukee, Wisconsin

Correspondence: Dr. Alison J. Kriegel, Department of Physiology, Medical College of Wisconsin, 8701 Watertown Plank Road, Milwaukee, WI 53226. Email: akriegel@mcw.edu

CKD now afflicts >15% of the US adult population (6). New diagnostic and treatment strategies for CKD are urgently needed. Assessment of urine-excreted biomarkers has long been a diagnostic and prognostic cornerstone of kidney disease. Rapid technologic advances are changing this field. Old standbys such as urine albumin are now being supplemented by new-age, "omics-based" (*e.g.*, transcriptomics), urine-excreted biomarker analysis. Many such studies focused on extracellular vesicles, especially exosomes, and microvesicles, and provided novel insight into renal pathophysiology. We know the presence of our CKD rat LRT-EVs to temporally coincide with marked exacerbation of renal pathology (1). On the basis of these observations, we hypothesized that LRT-EVs are excreted in the urine and contain proteins essential to healthy renal function. Toward this, and while mindful of insightful omics-based extracellular vesicle analysis from others, we performed a tandem mass spectrometry (MS/MS) proteomic analysis of LRT-EVs we isolated from CKD rat urine. We found LRT-EVs to contain a wide array of tubule proteins. Many of these were PT epithelial proteins that, upon disruption, are known to contribute to hallmarks of renal disease. This study provides needed information upon hitherto poorly characterized, renal pathology–associated LRT-EVs. Because LRT-EVs contain proteins essential to healthy renal function, their formation and excretion represents a potential, newly described mechanism of renal pathology.

Materials and Methods

Animal Model

All animal protocols were approved by the Medical College of Wisconsin Institutional Animal Care and Use Committee and performed in compliance with the National Institutes of Health (NIH) Guide for the Care and Use of Laboratory Animals. Male Sprague-Dawley rats (Envigo, Madison, WI) were maintained on 0.4% sodium chloride chow (AIN-76A Purified Rodent Diet; Dyets Inc., Bethlehem, PA) and water *ad libitum*, under a 12-hour light cycle. At 10 weeks of age, animals underwent a sham or 5/6Nx operation, as described previously (1,4). In brief, rats were anesthetized (50 mg/kg ketamine, 8 mg/kg xylazine, and 5 mg/kg acepromazine), and the entire right kidney and left kidney poles were removed by surgical excision. Gelfoam coagulant was applied to resected surfaces. All subsequent rat data collection was performed 10 weeks after the 5/6Nx or sham surgery.

Tissue Collection and Histology

Tissues were excised from anesthetized animals and immediately immersion fixed in 10% formalin. Kidneys were processed, paraffin-embedded, sectioned (4 μm), and stained with Masson trichrome by the Children's Research Institute Histology Core at the Medical College of Wisconsin. Light microscopy was performed using an Eclipse E-400 microscope (Nikon). TUNEL staining was performed following the manufacturer's instructions (Click-iT Plus TUNEL Assay), with DNAase I pretreatment as a positive control (Thermo Fisher). Mounting medium with 4′,6-diamidino-2-phenylindole (DAPI; Vector Laboratories) was used to label nuclei. Imaging was performed on a Nikon A1-R laser scanning confocal microscope. Immunohistochemistry for megalin was performed as previously described (7), with 1:50 megalin antibody (AB184676; Abcam) and 1:100 Texas Red–labeled anti-mouse antibody (T-862, 1:100; Invitrogen). Immunohistochemistry for sodium-hydrogen antiporter 3 (NHE3; also known as SLC9A3) was performed in the same manner, except with 1:50 NHE3 antibody (MABN1813; Millipore Sigma). Imaging was performed with an Eclipse 80i microscope (Nikon) or Nikon A1-R confocal microscope. Histologic sections of PTs, stained with Masson trichrome, from sham and 5/6Nx rats were assessed for the presence of LRT-EVs. This analysis was performed on histologic sections acquired from separate cohorts of sham and 5/6Nx rats at 2, 4, 5, 7, and 10 weeks postsurgery.

LRT-EV Isolation and Diameter Measurement

Sham-operated and 5/6Nx rats (n=3 per group) were housed in wire-bottom metabolic cages, and urine was collected into ice-immersed conical tubes for 24 hours. All subsequent steps were performed at room temperature. Urine was filtered (70-μm mesh), and then centrifuged at 300 $\times$ g for 15 minutes (spin A). The resulting pellet was resuspended in 1 ml PBS and centrifuged again (spin B). The supernatant from both spins (A and B) was combined and centrifuged at 650 $\times$ g for 10 minutes (spin C), to remove any larger material or shed cells. The supernatant from spin C was centrifuged at 2000 $\times$ g for 10 minutes (spin D), to pellet the LRT-EV's. The pellet was then washed in 1 ml of PBS and centrifuged at 580 $\times$ g for 10 minutes (Spin E). An aliquot of this final isolate was inspected and imaged under light microscopy for the presence of LRT-EVs. No LRT-EVs were observed in samples fractionated from sham-operated rat urine. The LRT-EV isolation methodology is summarized in Supplemental Figure 1. The size of LRT-EVs from 5/6Nx rats was measured from the light-microscopy images using the Analyze Particles feature of FIJI software (free download: https://imagej.net/Fiji/Downloads).

Proteomic Sample Preparation and Analysis

The remaining LRT-EVs were transferred to a Dounce homogenizer and mechanically lysed on ice, followed by 30 minutes of water-bath sonication at room temperature, as previously described (8). Homogenized LRT-EVs were then buffer swapped (5×) and concentrated into 250 μl of 25 mM ammonium bicarbonate, pH 8.0, using 3K MWCO Amicon Ultrafiltration Units (Millipore), as described by the manufacturer's protocol. The concentrated LRT-EV protein fractions then had 0.1% of the MS-compatible RapiGest surfactant (Waters) added, followed by incubation on ice for 10 minutes. Samples were then reduced (10 mM dithiothreitol for 30 minutes at 37°C), alkylated (20 mM iodoacetamide for 30 minutes in the dark at room temperature), and digested with Trypsin Gold (Promega), as previously described (8–10). After protein digestion, all samples were desalted/concentrated using OMIX C18 zip-tips (Varian), according to the manufacturer's protocol, and prepared for liquid chromatography–MS/MS analysis as previously described (8–10). Peptides were separated on a NanoAcquity UPLC system (Waters) with a C18 (Phenomenex) column with a 240-minute gradient (2%–98% acetonitrile) and analyzed with a LTQ-Orbitrap Velos MS (Thermo Fisher), as previously described (8,10,11).

The MS/MS spectral data were searched against the rodent UniProtKB protein databases in Mascot and SEQUEST algorithms, followed by comparative analysis using the Visualize proteomic software (8,12). Within the software, preference was given to rat, and the Mascot/SEQUEST matches were combined for each run using the combine search function, which matches each scan to the best spectral match from either algorithm to ensure no redundancy. Filters were applied for each search, including a Visualize $P>0.85$ (false discovery rate<5%). All biologic replicates ($N=3$ with two technical replicates of each; six total runs) were then combined in Visualize where a peptide filter of two or more peptides and a scan count filter of six was applied. The unique proteins detected in the experiments were uploaded to Ingenuity Pathway Analysis, using the UniProt accession number for subsequent categorization of proteins by known cellular location and function/type (7). The MS proteomics data have been deposited to the ProteomeXchange Consortium, *via* the PRIDE partner repository, with the dataset identifiers PXD019207 and 10.6019/PXD019207 (13).

Statistical Analysis

Histologic assessment for the presence of LRT-EVs in PTs (Figure 1D) are represented as average±SEM. These data were not normally distributed, as assessed by the Shapiro–Wilk test. Therefore, the nonparametric Mann–Whitney test was used to determine the presence of significant differences ($P<0.05$) between groups.

Results

We observed vesicles budding from PTs 10 weeks after 5/6Nx surgery (Figure 1A), a time when these rats exhibit substantial pathology, including tubular damage, proteinuria, and cardiovascular dysfunction (1). Sham-operated rats had intact brush borders and lacked lumenal vesicles. In 5/6Nx rats, the PT epithelial cells in regions of large vesicle production had intact nuclei upon visual inspection, were not TUNEL positive, and no TUNEL or DAPI signal was detected within the vesicles (Figure 1B), suggesting these vesicles are not apoptotic bodies. We isolated LRT-EVs (Figure 1C) from 5/6Nx rat urine using a purpose-

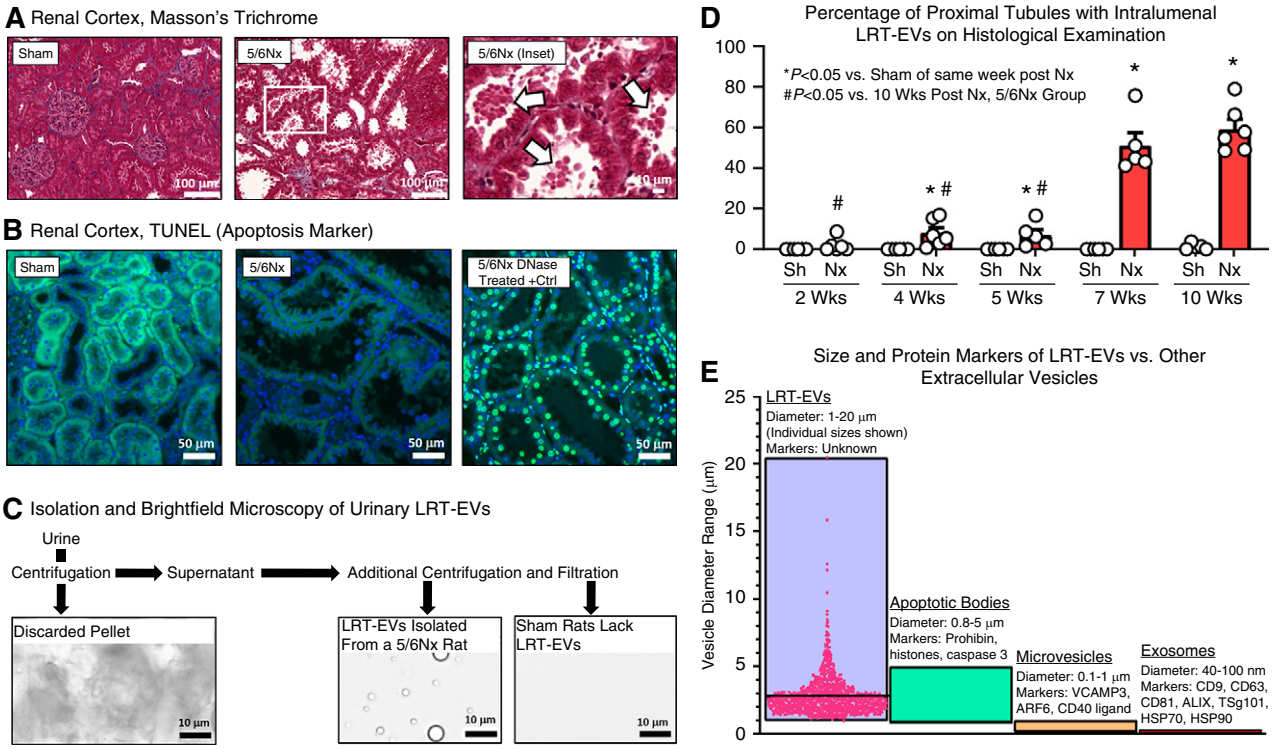

Figure 1. | Large renal tubular extracellular vesicles (LRT-EVs) spontaneously form in 5/6Nx but not sham-operated rats, are easily visible upon routine histological assessment, and are urine-excreted. (A) Examination of renal cortical tissue collected from 5/6 nephrectomy (5/6Nx) and sham-operated controls 10 weeks postsurgery. 5/6Nx rats exhibited extensive brush-border loss and the presence of large renal tubule extracellular vesicles (LRT-EVs) in proximal tubule lumens (arrows). (B) Terminal deoxynucleotidyl transferase–mediated digoxigenin-deoxyuridine nick-end labeling (TUNEL) indicates apoptosis by labeling DNA double-strand breaks. Kidney sections from sham-operated (sham; left) and 5/6Nx (center) rats were TUNEL negative (488 nm autofluorescence, green; 4′,6-diamidino-2-phenylindole [DAPI], blue). Importantly, the large vesicles within the lumen and the nuclei of the cells producing the vesicles were both TUNEL negative. A section treated with DNase (right) serves as a positive control for the assay (DAPI in blue colocalized with TUNEL in bright green). (C) These vesicles were isolated from 5/6Nx rat urine through a sequence of filtration and centrifugation (see Supplemental Figure 1 for detailed methodology). Sham rat urine lacked LRT-EVs. (D) Proximal tubules were scored for the presence of LRT-EVs in separate cohorts of sham and 5/6Nx rats at 2, 4, 5, 7, and 10 weeks postsurgery. Each dot represents one animal. (E) The size, as measured by microscopic analysis, and lack of apoptotic markers suggest these vesicles (LRT-EVs) represent a unique category of urine-excreted, extracellular vesicle, prompting proteomic analysis to characterize their composition. A subset of published diameters and protein markers of exosomes, microvesicles, and apoptotic bodies are represented here (5,14,15). Individual LRT-EV diameter measurements are shown; horizontal bar equals average. Nx, 5/6 Nx; Sh, sham.

developed, filtration and differential centrifugation methodology (Supplemental Figure 1). We histologically determined the presence of LRT-EVs in PTs in sham and 5/6Nx rats at 2, 4, 5, 7, and 10 weeks postsurgery (Figure 1D). The presence of LRT-EVs in PTs was time dependent. At 2 weeks postsurgery, 2%±1% (average±SEM) of 5/6Nx PTs had LRT-EVs; at 4 weeks, 8%±3%; at 5 weeks, 7%±3%; at 7 weeks, 51%±6%; and at 10 weeks, 59%±5%. The PTs of sham-operated rats had virtually no LRT-EVs at any of those time points. Microscopic image analysis of LRT-EVs isolated from urine at 10 weeks postsurgery revealed them to be circular in shape (in the two-dimensional images), with an average diameter ± SD of 2.8 ± 1.5 μm, and median diameter of 2.5 μm. It is possible that LRT-EVs of a larger diameter were eliminated as part of the isolation methodology. LRT-EV size and protein markers render them distinct from exosomes, microvesicles, and apoptotic bodies (Figure 1E).

Proteomic analysis of isolated LRT-EVs detected 447 proteins (Supplemental Table 1). These proteins were of diverse functionality and derive from numerous cellular locations (Figure 2A). Of the total proteins, 46% were cytoplasmic proteins, 24% were extracellular space proteins, 7% were nuclear proteins, and 20% were plasma membrane proteins. Proteins within these respective cellular domains were subdivided by functionality. Subgroups included the following: transporters, enzymes, ion channels, kinases, peptidases, transcriptional regulators, phosphatases, G protein–coupled receptors, cytokines, and transmembrane receptors (Table 1). The LRT-EVs contained megalin (LDL-related protein 2; LRP2) in relatively high quantities. Megalin is a PT-microvilli reabsorption mediator of numerous ligands, including vitamin carrier proteins, lipoproteins, hormones, enzymes, immune-related proteins, and select drugs and toxins (16). Consistent with the proteomics, immunohistochemical analysis indicated the presence of megalin within LRT-EVs (Figure 2B). We also observed that megalin was abundant throughout the PT in 5/6Nx rats, but its intracellular localization was abnormally distributed. NHE3 (SL9A3) is a PT protein that was not identified in LRT-EVs. Consistent with these data, immunohistochemical analysis indicated robust NHE3 expression in sham-operated rat PT epithelial cells, reduced expression in PT epithelial cells of 5/6Nx rats, and no expression in LRT-EVs (Figure 2C).

Discussion

We demonstrate there to be innumerable, protein-laden, LRT-EVs in the PTs and urine of 5/6Nx rats 10 weeks postsurgery. LRT-EVs house proteins essential to PT reabsorption. The importance of PT brush-border reabsorption is made clinically evident by the severity of the genetic diseases in which it is comprised (*e.g.*, Dent disease, Fanconi syndrome). The loss of numerous functionally important proteins through LRT-EV formation in a CKD-like model of chronic renal stress/insufficiency has not been characterized. These shed proteins are varied in function, and, therefore, their loss likely contributes to a spectrum of CKD-related phenotypes. The effect size of these lost proteins on cellular function is likely dependent on a complex relationship between the magnitude of protein loss, cellular demand for that protein's function, and the cell's ability to compensate through translational replacement and/or compensatory mechanisms. Loss of PT proteins has been described in other models of renal injury (3,17). It is possible this protein loss is caused, in part, by LRT-EV formation and excretion, although additional studies would be required to confirm this.

LRT-EV size, lack of protein markers specific to other extracellular vesicles, and presence only in specific pathologic settings, render them distinct from relatively well-characterized urine extracellular vesicles such as exosomes, microvesicles, and apoptotic bodies. To the best of our knowledge, this is the first, explicit description of LRT-EVs. Although much work remains to more fully characterize LRT-EVs, this study enables us to draw several inferences about them. First, LRT-EVs are likely derived, at least in part, from the PT epithelium. This is suggested by their absence in the Bowman's capsule; their presence in the PT; their temporal correspondence to PT brush-border loss; and their containment of many PT-specific proteins, including aquaporin 1 (AQP1), cubilin, and megalin. Second, LRT-EV presence in CKD 5/6Nx rats, but not in sham-operated rats, may suggest LRT-EVs lack membership within the "healthy" tubule extracellular vesicle milieu, but rather exist consequent to pathology. In this respect, LRT-EVs bear resemblance to oncosomes and exophers. Oncosomes are very large extracellular vesicles (1–10 μm), carry oncogenic proteins, and have only been observed in association with cancer (18,19). Exophers, which are also large (4 μm), are extracellular vesicles produced by *Caenorhabditis elegans* neurons only under specific conditions of neuronal stress. Exophers appear to be a means by which these neurons package and jettison neurotoxic components (20). Not only are LRT-EVs similar to oncosomes and exophers in size, but also in their derivation from a particular tissue type only under specific pathologic conditions. In contrast, exosomes and microvesicles are found in urine from healthy individuals. Third, urine exosomes, microvesicles, and apoptotic bodies are each associated with specific protein markers. These markers often reflect the mechanism of their respective vesicle's formation. For example, exosomes are endosomal in origin and contain protein markers (*e.g.*, TSG101, ALIX) associated with the endosomal system (5,14,15). Similarly, microvesicles form through outward budding of the plasma membrane; some proteins involved in this process, such as ARF6, are microvesicle protein markers (14). Apoptotic bodies are associated with markers of apoptosis, such as caspase 3 (14,15). The protein markers of exosomes, microvesicles, and apoptotic bodies were largely absent from LRT-EVs, perhaps suggesting LRT-EVs have a formation mechanism distinct from those extracellular vesicles.

Many LRT-EV proteins are important for maintenance of cellular homeostasis (Figure 3A). For example, regucalcin is an important nuclear and cytoplasmic calcium ion regulator. Superoxide dismutase family members SOD1 and SOD3 are critical to the cellular response to reactive oxygen species. Voltage-dependent anion-selective channels VDAC1 and VDAC2, and ATP synthase subunits (ATP5F1A, ATP5F1B, ATP5PB) play key roles in mitochondrial energetics. Loss of such proteins may reduce the PT's capacity for reabsorption, albeit indirectly. LRT-EVs also contained many proteins directly involved in reabsorption (Figure 3B).

Table 1. Summary of protein diversity in large renal tubular extracellular vesicles

Location	Category	UniProt/Swiss-Prot/GenPept Accession	Protein Symbol	Scan Count	Peptide Count	Entrez Gene Name
Cytoplasmic	Enzymes	P19468	GSH1	25	260	Glutamate-cysteine ligase catalytic subunit
		P04764	ENOA	17	139	Enolase 1
		P07632	SODC	8	109	SOD1
	Ion channels	P81155	VDAC2	10	44	Voltage dependent anion channel 2
		Q9Z2L0	VDAC1	6	22	Voltage dependent anion channel 1
	Kinases	Q4KLZ6	TKFC	16	74	Triokinase and FMN cyclase
		P16617	PGK1	10	40	Phosphoglycerate kinase 1
		P07379	PCKGC	8	30	Phosphoenolpyruvate carboxykinase 1
	Peptidases	P00758	KLK1	8	165	Kallikrein 1
		P00787	CATB	12	147	Cathepsin B
		P16675	PPGB	10	125	Cathepsin A
	Phosphatases	P25113	PGAM1	8	36	Phosphoglycerate mutase 1
		P20611	PPAL	8	27	Acid phosphatase 2, lysosomal
		Q91YE9	5NT1B	8	18	5′-Nucleotidase, cytosolic 1B
	Transporters	P55054	FABP9	10	60	Fatty acid binding protein 9
		P19511	AT5F1	3	59	ATP synthase peripheral stalk-membrane subunit b
		P10719	ATPB	14	44	ATP synthase F1 subunit β
Extracellular	Cytokines	P08721	OSTP	7	86	Secreted phosphoprotein 1
		Q9CPT4	MYDGF	3	14	Myeloid-derived growth factor
		P06684	CO5	4	12	Complement C5
	Growth factors	P07522	EGF	44	590	EGF
		P01015	ANGT	15	189	Angiotensinogen
		P23785	GRN	7	98	Granulin precursor
	Other proteins	P17475	A1AT	40	2659	Serpin family A member 1
		P05545	SPA3K	32	2252	Serine protease inhibitor A3K precursor
		P27590	UROD	24	1724	Uromodulin
	Peptidases	Q01177	PLMN	58	1172	Plasminogen
		P01026	CO3	78	949	Complement C3
		P06866	HPT	24	401	Haptoglobin
	Transporters	P02770	ALBU	9	16,638	Albumin
		P12346	TRFE	65	3405	Transferrin
		P14046	MUG1	74	1583	Murinoglobulin 1

Table 1. (Continued)

Location	Category	UniProt/Swiss-Prot/GenPept Accession	Protein Symbol	Scan Count	Peptide Count	Entrez Gene Name
Plasma membrane	Enzymes	P07314	GGT1	21	324	γ-Glutamyltransferase 1
		P97675	ENPP3	10	23	Ectonucleotide pyrophosphatase/phosphodiesterase 3
		Q8CFN2	CDC42	3	19	Cell division cycle 42
	G protein–coupled receptors	Q3KRC4	GPRC5C	2	8	G protein–coupled receptor class C group 5 member C
	Ion channels	Q9Z0W7	CLIC4	10	64	Chloride intracellular channel 4
		Q9Z0Y8	CACNA1I	2	7	Calcium voltage-gated channel subunit α1 I
		Q91YD4	TRPM2	2	6	Transient receptor potential cation channel subfamily M member 2
	Kinases	Q01279	EGFR	4	9	EGF receptor
	Other proteins	P31977	EZRI	28	241	Ezrin
		Q9R0T4	CADH1	13	204	Cadherin 1
		Q9JJ19	NHRF1	25	131	SLC9A3 regulator 1
	Peptidases	P15684	AMPN	30	418	Alanyl aminopeptidase, membrane
		P07861	NEP	34	361	Membrane metalloendopeptidase
		P14740	DPP4	31	289	Dipeptidyl peptidase 4
	Transmembrane proteins	P07151	B2MG	8	143	β-2-Microglobulin
		O70244	CUBN	17	58	Cubilin
		Q63257	IL4RA	4	48	IL-4 receptor
	Transporters	P98158	LRP2	106	651	LDL receptor-related protein 2/megalin
		Q64319	SLC3A1	31	427	Solute carrier family 3 member 1
		Q9JJ40	NHRF3	20	152	PDZ domain-containing 1
		P29975	AQP1	8	151	Aquaporin 1
		P15083	PIGR	21	134	Polymeric Ig receptor
		Q62687	S6A18	12	86	Solute carrier family 6 member 18
		Q63424	S15A2	16	59	Solute carrier family 15 member 2
		Q9WTW7	S23A1	11	43	Solute carrier family 23 member 1
		Q80W57	ABCG2	9	33	ATP binding cassette subfamily G member 2
		P50516	VATA	9	32	ATPase H^+ transporting V1 subunit A

This table summarizes the three most abundant proteins (by scan count and if present) within each functional category (type) of select cellular locations identified by Ingenuity Pathway Analysis. The ten most abundant transport proteins in the plasma membrane are indicated. UniProt accession numbers, protein symbols, and Entrez gene name are also provided. See Supplemental Table 1 for a complete list of Ingenuity Pathway Analysis–identified protein location/types. SLC9A3, sodium-hydrogen antiporter 3; FMN, flavin mononucleotide; H^+, hydrogen ion.

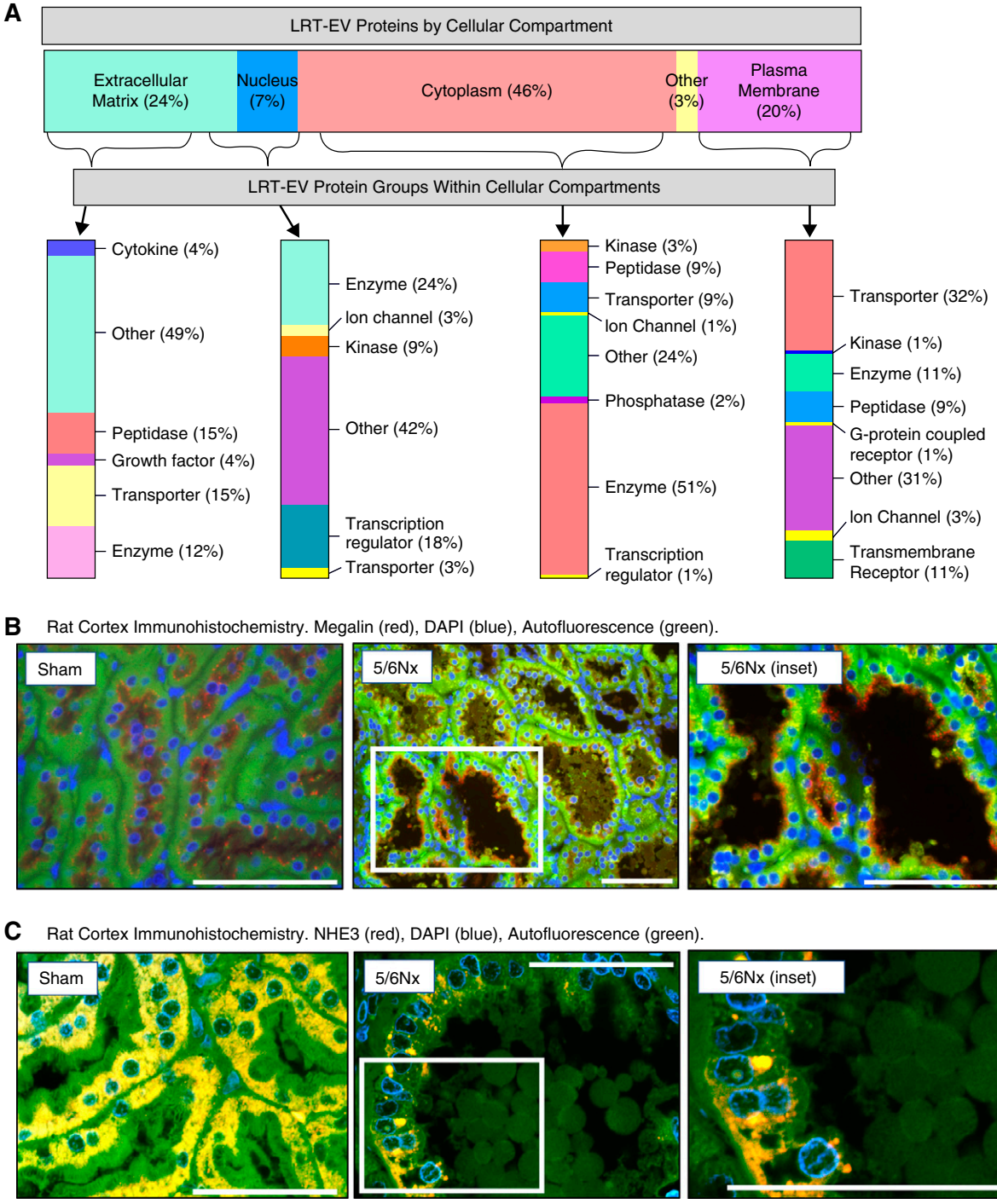

Figure 2. | Proteomic analysis revealed LRT-EVs to contain proteins derived from numerous cellular compartments and of variable functional class. (A) Proteins identified through tandem mass spectrometry data analysis (N=3 with two technical replicates of each; six runs total), and meeting a minimum scan count of six and peptide count of two, were uploaded to Ingenuity Pathway Analysis to categorize these proteins based on cellular compartment and protein type/function. The percentage of identified LRT-EV proteins per cellular compartment (location) is depicted on the horizontal bar at the top. The proteins within each cellular compartment are then subcategorized by type, with percentage within each compartment indicated at the right of the vertical bars. (B) Proteomic analysis identified the plasma membrane transporter megalin in LRT-EVs. Representative immunohistochemistry of kidney tissues collected 10 weeks postsurgery show presence of megalin (red) localized at the base of the brush border on the apical membrane in sham-operated (sham) rats. In 5/6Nx rats, megalin can be seen in LRT-EVs that are within the tubule lumen and LRT-EVs emerging from the proximal tubule cells. The distribution of megalin is diffuse (yellow) or absent in some tubular cells. Image on right is an inset from center image. DAPI, blue; autofluorescence at 455 nm, green. Scale bar, 100 μm. (C) Proteomic analysis failed to detect sodium-hydrogen antiporter 3 (NHE3) in LRT-EVs. Immunohistochemistry of kidney tissue collected 10 weeks postsurgery shows the presence of NHE3 (red) in sham and 5/6Nx rat proximal tubule epithelial, but not in LRT-EVs. DAPI, blue; autofluorescence at 455 nm, green. Scale bar, 50 μm.

Their collective loss likely contributes to a spectrum of CKD-related phenotypes. Our proteomic analysis identified 16 proteins of the solute carrier family—plasma membrane transporters that facilitate reabsorption of many solutes. Among them were SLC3A1 and SLC34A1, functional loss of which is associated with cystinuria and phosphaturia, respectively (21,22). Proteomics identified sodium-glucose cotransporters (SLC5A1 and SLC5A2) in LRT-EVs. Their functional inhibition is associated with glucosuria, which is reported to occur with progressive brush-border loss (3). Megalin and cubilin, both found within LRT-EVs, are receptors that facilitate reabsorption of a wide variety of ligands, including proteins. LRT-EVs contained five subunits of vacuolar ATPase (ATP6V1A, ATP6V1B2, ATP6V0D1, ATP6V0C, and ATP6V1E1), a proton pump that is in PT epithelia and in distal tubule intercalated cells (23). Vacuolar ATPase regulates organelle pH and endocytic reabsorption of filtered proteins, among other functions (24,25). Also lost in urine-excreted LRT-EVs was G protein–coupled receptor family C group 5 member C (GPRC5C). Gprc5c-knockout mice have reduced blood pH and elevated urine pH (26). LRT-EVs contained AQP1, an important mediator of water balance. AQP1 loss impairs the kidney's ability to concentrate urine (27). LRT-EVs contained sodium-potassium ATPase (Na^+/K^+-ATPase) subunit α 1, a primary component of the basolateral Na^+/K^+-ATPase. The transmembrane Na^+/K^+-ATPase is responsible for generating the electrochemical gradient that facilitates virtually all energy-dependent tubular reabsorption in the PT.

Some PT proteins abundantly expressed in health were identified in LRT-EVs (*e.g.*, SLC2A1 and SLC34A1), whereas others were not, such as SLC9A3 (NHE3). This could indicate that inclusion of specific proteins into LRT-EVs is not strictly on the basis of abundance. It may also reflect intrinsic protein-expression changes consequent of pathology. For example, NHE3 expression, highly expressed in health, is significantly reduced only 2 weeks after 5/6Nx in rats (28,29). Our immunohistochemistry analysis of NHE3 expression (Figure 2C) is consistent with these previous studies. Thus, LRT-EVs may lack NHE3, and other PT proteins abundantly expressed in health, due to a pathology-related reduction in expression. Interestingly, NHE3-regulator 1 (NHE3R1) was identified in LRT-EVs. NHE3R1 is involved in NHE3 intracellular trafficking (30). Thus, loss of NHE3R1 to LRT-EVs may have contributed to the differences in NHE3 expression between sham and 5/6Nx rat PT epithelia. From this study, we are unable to determine how and why specific proteins were included in LRT-EVs while others were not. Inclusion likely depends upon a complex amalgam of regulated and stochastic factors.

Several studies have made important contributions to our knowledge of the PT and urinary proteome (31–33). The "shotgun" proteomics-based analysis of 5/6Nx LRT-EVs provided here adds to our understanding of renal tubular pathophysiology. Hypothesis-driven investigations of LRT-EV production and characteristics in different disease states and model systems may provide deeper understanding of changes that occur during CKD progression. This study had a number of limitations. First, the marked increase in LRT-EV formation and excretion that occurred between week 5 and 7 postsurgery coincided with the timing of a sharp decline in renal function in this model, including elevations in proteinuria, and an abrupt increase in histologic evidence of proximal tubule pathology, including hypertrophy and dilation (1). Despite this, we are unable, from this study, to determine conclusively that LRT-EVs are a pathogenic mechanism of CKD. However, the fact that they house functionally important tubule proteins suggests they are, at a minimum, formed during a period of rapid worsening of renal function in the 5/6Nx model of CKD. Second, many LRT-EV proteins were specific to the PTs, but others were not. For example, LRT-EVs contained FABP3, which, in health, is expressed in greater abundance in distal tubules than PTs (34), and is considered a urinary biomarker of distal tubule damage (35). Although PTs appear to be the predominate site of LRT-EV formation, LRT-EVs may be generated at additional sites. Third, we performed our proteomic analysis on LRT-EVs collected from 5/6Nx rats 10 weeks postsurgery. The LRT-EV proteome likely varies with renal injury type and with advances (or retreats) in disease progression.

In conclusion, the 5/6Nx rat model of CKD spontaneously produces LRT-EVs that are excreted in the urine. Our proteomic analysis indicates LRT-EVs contain a wide assortment of proteins, including those specific to the PT epithelium such as transporters, enzymes, transmembrane receptors, and endocytic receptors (Figure 4). This study adds to the rapidly growing field of omics-based, renal disease, extracellular-vesicle analysis. Therapies designed to limit LRT-EV formation may improve renal function. Loss of important tubule proteins *via* excretion of LRT-EVs may represent an underappreciated pathogenic mechanism of renal disease.

Disclosures

All authors have nothing to disclose.

Funding

This research was supported by American Heart Association grant 13SDG17100095, NIH National Center for Advancing Translational Sciences grant 8UL1TR000055, and NIH National Heart, Lung, and Blood Institute grant R01HL128332 (to A. Kriegel).

Author Contributions

R. Adam, B. Hoffmann, and A. Kriegel wrote the original draft and were responsible for formal analysis and validation; R. Adam and A. Kriegel were responsible for data curation; R. Adam, A. Kriegel, M. Paterson, and L. Wardecke were responsible for methodology; R. Adam and L. Wardecke were responsible for investigation; A. Kriegel conceptualized the study and was responsible for funding acquisition, project administration, supervision, and visualization; and all authors reviewed and edited the manuscript.

Supplemental Material

This article contains the following supplemental material online at http://kidney360.asnjournals.org/lookup/suppl/doi:10.34067/KID.K3602020000121/DCSupplemental.

Supplemental Table 1. List of LRT-EV proteins detected by our proteomic analysis and their IPA-identified cellular location and function.

Supplemental Figure 1. LRT-EV isolation methodology.

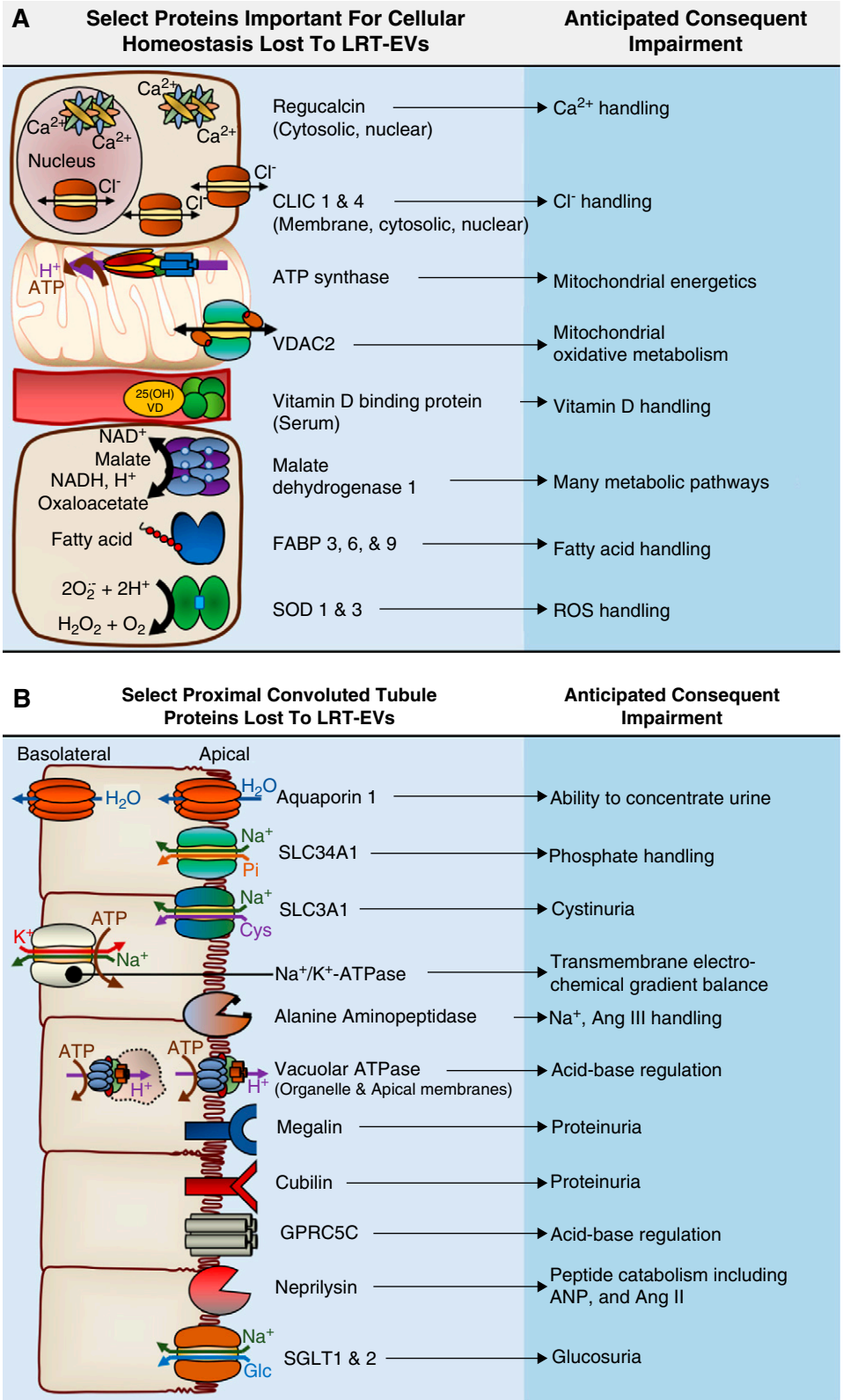

Figure 3. | Proteomic analysis revealed LRT-EVs to contain proteins derived from numerous cellular compartments and of variable functional class. 25(OH)VD, 25-hydroxyvitamin D; Ang II, angiotensin II; Ang III, angiotensin III, ANP, atrial natriuretic peptide; Ca^{2+}, calcium ion; Cl^{-}, chloride ion; CLIC, chloride intracellular channel protein; Cyst, cystine, FABP, fatty acid-binding protein; GPRC5C, G-protein coupled receptor family C group 5 member C; H^{+}, hydrogen ion; H_2O_2, hydrogen peroxide; K^{+}, potassium ion; Na^{+}, sodium ion; O_2, oxygen; Pi, inorganic phosphate; ROS, reactive oxygen species; SGLT, sodium-glucose cotransporter; SLC; solute carrier family member; SOD, superoxide dismutase, VDAC, voltage-dependent anion channel.

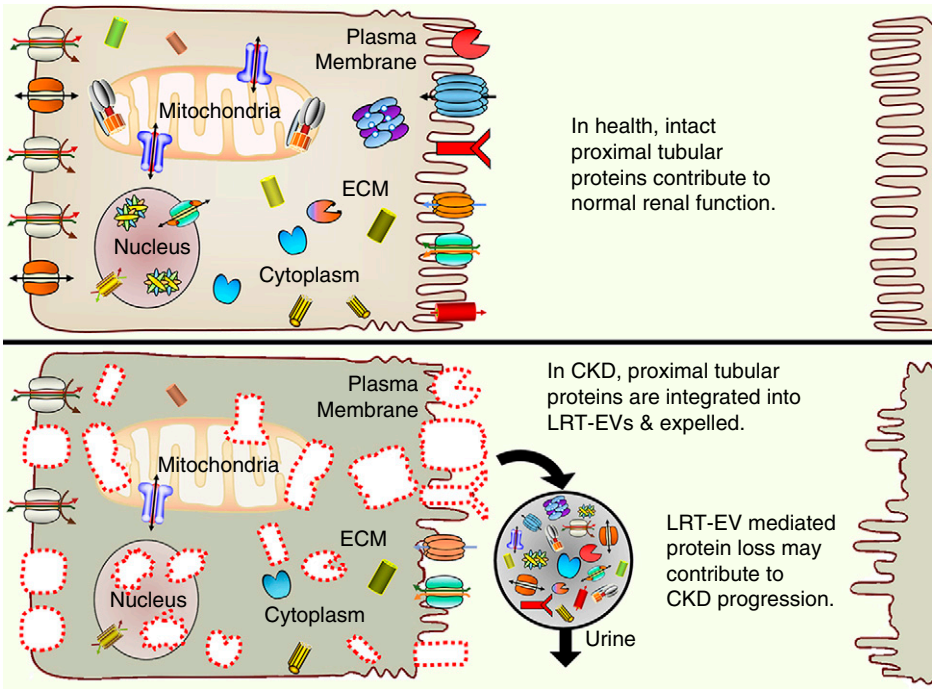

Figure 4. | Proteomic analysis revealed LRT-EVs to contain proteins derived from numerous cellular compartments and of variable functional class.

References

1. Chuppa S, Liang M, Liu P, Liu Y, Casati MC, Cowley AW, Patullo L, Kriegel AJ: MicroRNA-21 regulates peroxisome proliferator-activated receptor alpha, a molecular mechanism of cardiac pathology in cardiorenal syndrome type 4. *Kidney Int* 93: 375–389, 2018 10.1016/j.kint.2017.05.014
2. Fujigaki Y, Tamura Y, Nagura M, Arai S, Ota T, Shibata S, Kondo F, Yamaguchi Y, Uchida S: Unique proximal tubular cell injury and the development of acute kidney injury in adult patients with minimal change nephrotic syndrome. *BMC Nephrol* 18: 339, 2017 10.1186/s12882-017-0756-6
3. Takaori K, Nakamura J, Yamamoto S, Nakata H, Sato Y, Takase M, Nameta M, Yamamoto T, Economides AN, Kohno K, Haga H, Sharma K, Yanagita M: Severity and frequency of proximal tubule injury determines renal prognosis. *J Am Soc Nephrol* 27: 2393–2406, 2016 10.1681/ASN.2015060647
4. Paterson MR, Geurts AM, Kriegel AJ: miR-146b-5p has a sex-specific role in renal and cardiac pathology in a rat model of chronic kidney disease. *Kidney Int* 96: 1332–1345, 2019 10.1016/j.kint.2019.07.017
5. Merchant ML, Rood IM, Deegens JKJ, Klein JB: Isolation and characterization of urinary extracellular vesicles: Implications for biomarker discovery. *Nat Rev Nephrol* 13: 731–749, 2017 10.1038/nrneph.2017.148
6. Ceters for Disease Control and Prevention: Chronic Kidney Disease (CKD) surveillance system. Available at: http://nccd.cdc.gov/CKD. Accessed September 3, 2020
7. Kriegel AJ, Terhune SS, Greene AS, Noon KR, Pereckas MS, Liang M: Isomer-specific effect of microRNA miR-29b on nuclear morphology. *J Biol Chem* 293: 14080–14088, 2018 10.1074/jbc.RA117.001705
8. Freed JK, Durand MJ, Hoffmann BR, Densmore JC, Greene AS, Gutterman DD: Mitochondria-regulated formation of endothelium-derived extracellular vesicles shifts the mediator of flow-induced vasodilation. *Am J Physiol Heart Circ Physiol* 312: H1096–H1104, 2017 10.1152/ajpheart.00680.2016
9. Hoffmann BR, El-Mansy MF, Sem DS, Greene AS: Chemical proteomics-based analysis of off-target binding profiles for rosiglitazone and pioglitazone: Clues for assessing potential for cardiotoxicity. *J Med Chem* 55: 8260–8271, 2012 10.1021/jm301204r
10. Hoffmann BR, Wagner JR, Prisco AR, Janiak A, Greene AS: Vascular endothelial growth factor-A signaling in bone marrow-derived endothelial progenitor cells exposed to hypoxic stress. *Physiol Genomics* 45: 1021–1034, 2013 10.1152/physiolgenomics.00070.2013
11. Kaczorowski CC, Stodola TJ, Hoffmann BR, Prisco AR, Liu PY, Didier DN, Karcher JR, Liang M, Jacob HJ, Greene AS: Targeting the endothelial progenitor cell surface proteome to identify novel mechanisms that mediate angiogenic efficacy in a rodent model of vascular disease. *Physiol Genomics* 45: 999–1011, 2013 10.1152/physiolgenomics.00097.2013
12. Halligan BD, Greene AS: Visualize: A free and open source multifunction tool for proteomics data analysis. *Proteomics* 11: 1058–1063, 2011 10.1002/pmic.201000556
13. Perez-Riverol Y, Csordas A, Bai J, Bernal-Llinares M, Hewapathirana S, Kundu DJ, Inuganti A, Griss J, Mayer G, Eisenacher M, Pérez E, Uszkoreit J, Pfeuffer J, Sachsenberg T, Yilmaz S, Tiwary S, Cox J, Audain E, Walzer M, Jarnuczak AF, Ternent T, Brazma A, Vizcaíno JA: The PRIDE database and related tools and resources in 2019: Improving support for quantification data. *Nucleic Acids Res* 47: D442–D450, 2019 10.1093/nar/gky1106
14. Akers JC, Gonda D, Kim R, Carter BS, Chen CC: Biogenesis of extracellular vesicles (EV): Exosomes, microvesicles, retrovirus-like vesicles, and apoptotic bodies. *J Neurooncol* 113: 1–11, 2013 10.1007/s11060-013-1084-8
15. Barreiro K, Holthofer H: Urinary extracellular vesicles. A promising shortcut to novel biomarker discoveries. *Cell Tissue Res* 369: 217–227, 2017 10.1007/s00441-017-2621-0
16. Nielsen R, Christensen EI, Birn H: Megalin and cubilin in proximal tubule protein reabsorption: From experimental models to human disease. *Kidney Int* 89: 58–67, 2016 10.1016/j.kint.2015.11.007
17. Rangarajan S, Rezonzew G, Chumley P, Fatima H, Golovko MY, Feng W, Hua P, Jaimes EA: COX-2-derived prostaglandins as mediators of the deleterious effects of nicotine in chronic kidney disease. *Am J Physiol Renal Physiol* 318: F475–F485, 2020 10.1152/ajprenal.00407.2019

18. Jaiswal R, Sedger LM: Intercellular vesicular transfer by exosomes, microparticles and oncosomes - implications for cancer biology and treatments. *Front Oncol* 9: 125, 2019 10.3389/fonc.2019.00125
19. Minciacchi VR, You S, Spinelli C, Morley S, Zandian M, Aspuria PJ, Cavallini L, Ciardiello C, Reis Sobreiro M, Morello M, Kharmate G, Jang SC, Kim DK, Hosseini-Beheshti E, Tomlinson Guns E, Gleave M, Gho YS, Mathivanan S, Yang W, Freeman MR, Di Vizio D: Large oncosomes contain distinct protein cargo and represent a separate functional class of tumor-derived extracellular vesicles. *Oncotarget* 6: 11327–11341, 2015 10.18632/oncotarget.3598
20. Melentijevic I, Toth ML, Arnold ML, Guasp RJ, Harinath G, Nguyen KC, Taub D, Parker JA, Neri C, Gabel CV, Hall DH, Driscoll M: C. elegans neurons jettison protein aggregates and mitochondria under neurotoxic stress. *Nature* 542: 367–371, 2017 10.1038/nature21362
21. Iwaki T, Sandoval-Cooper MJ, Tenenhouse HS, Castellino FJ: A missense mutation in the sodium phosphate co-transporter Slc34a1 impairs phosphate homeostasis. *J Am Soc Nephrol* 19: 1753–1762, 2008 10.1681/ASN.2007121360
22. Livrozet M, Vandermeersch S, Mesnard L, Thioulouse E, Jaubert J, Boffa JJ, Haymann JP, Baud L, Bazin D, Daudon M, Letavernier E: An animal model of type A cystinuria due to spontaneous mutation in 129S2/SvPasCrl mice. *PLoS One* 9: e102700, 2014 10.1371/journal.pone.0102700
23. Stehberger PA, Schulz N, Finberg KE, Karet FE, Giebisch G, Lifton RP, Geibel JP, Wagner CA: Localization and regulation of the ATP6V0A4 (a4) vacuolar H+-ATPase subunit defective in an inherited form of distal renal tubular acidosis. *J Am Soc Nephrol* 14: 3027–3038, 2003 10.1097/01.ASN.0000099375.74789.AB
24. Marshansky V, Vinay P: Proton gradient formation in early endosomes from proximal tubules. *Biochim Biophys Acta* 1284: 171–180, 1996 10.1016/S0005-2736(96)00123-X
25. Sasaki Y, Nagai J, Kitahara Y, Takai N, Murakami T, Takano M: Expression of chloride channel, ClC-5, and its role in receptor-mediated endocytosis of albumin in OK cells. *Biochem Biophys Res Commun* 282: 212–218, 2001 10.1006/bbrc.2001.4557
26. Rajkumar P, Cha B, Yin J, Arend LJ, Păunescu TG, Hirabayashi Y, Donowitz M, Pluznick JL: Identifying the localization and exploring a functional role for Gprc5c in the kidney. *FASEB J* 32: 2046–2059, 2018 10.1096/fj.201700610RR
27. Ma T, Yang B, Gillespie A, Carlson EJ, Epstein CJ, Verkman AS: Severely impaired urinary concentrating ability in transgenic mice lacking aquaporin-1 water channels. *J Biol Chem* 273: 4296–4299, 1998 10.1074/jbc.273.8.4296
28. Kwon TH, Frøkiaer J, Fernández-Llama P, Maunsbach AB, Knepper MA, Nielsen S: Altered expression of Na transporters NHE-3, NaPi-II, Na-K-ATPase, BSC-1, and TSC in CRF rat kidneys. *Am J Physiol* 277: F257–F270, 1999
29. Nishihara K, Masuda S, Ji L, Katsura T, Inui K: Pharmacokinetic significance of luminal multidrug and toxin extrusion 1 in chronic renal failure rats. *Biochem Pharmacol* 73: 1482–1490, 2007 10.1016/j.bcp.2006.12.034
30. Cha B, Kenworthy A, Murtazina R, Donowitz M: The lateral mobility of NHE3 on the apical membrane of renal epithelial OK cells is limited by the PDZ domain proteins NHERF1/2, but is dependent on an intact actin cytoskeleton as determined by FRAP. *J Cell Sci* 117: 3353–3365, 2004 10.1242/jcs.01180
31. Gonzales PA, Pisitkun T, Hoffert JD, Tchapyjnikov D, Star RA, Kleta R, Wang NS, Knepper MA: Large-scale proteomics and phosphoproteomics of urinary exosomes. *J Am Soc Nephrol* 20: 363–379, 2009 10.1681/ASN.2008040406
32. Caterino M, Zacchia M, Costanzo M, Bruno G, Arcaniolo D, Trepiccione F, Siciliano RA, Mazzeo MF, Ruoppolo M, Capasso G: Urine proteomics revealed a significant correlation between urine-fibronectin abundance and estimated-GFR decline in patients with bardet-biedl syndrome. *Kidney Blood Press Res* 43: 389–405, 2018 10.1159/000488096
33. Wilmes A, Bielow C, Ranninger C, Bellwon P, Aschauer L, Limonciel A, Chassaigne H, Kristl T, Aiche S, Huber CG, Guillou C, Hewitt P, Leonard MO, Dekant W, Bois F, Jennings P: Mechanism of cisplatin proximal tubule toxicity revealed by integrating transcriptomics, proteomics, metabolomics and biokinetics. *Toxicol In Vitro* 30: 117–127, 2015 10.1016/j.tiv.2014.10.006
34. Maatman RG, Van Kuppevelt TH, Veerkamp JH: Two types of fatty acid-binding protein in human kidney. Isolation, characterization and localization. *Biochem J* 273: 759–766, 1991 10.1042/bj2730759
35. Meijer E, Boertien WE, Nauta FL, Bakker SJ, van Oeveren W, Rook M, van der Jagt EJ, van Goor H, Peters DJ, Navis G, de Jong PE, Gansevoort RT: Association of urinary biomarkers with disease severity in patients with autosomal dominant polycystic kidney disease: A cross-sectional analysis. *Am J Kidney Dis* 56: 883–895, 2010 10.1053/j.ajkd.2010.06.023

Received: March 11, 2020 **Accepted:** August 19, 2020